Supporting information

Sonochemical synthesis of cyclophosphazene bridged mesoporous organosilicas and their application in methyl orange, congo red and Cr(VI) removal

Pawan Rekha, Raeesh Muhammad and Paritosh Mohanty*

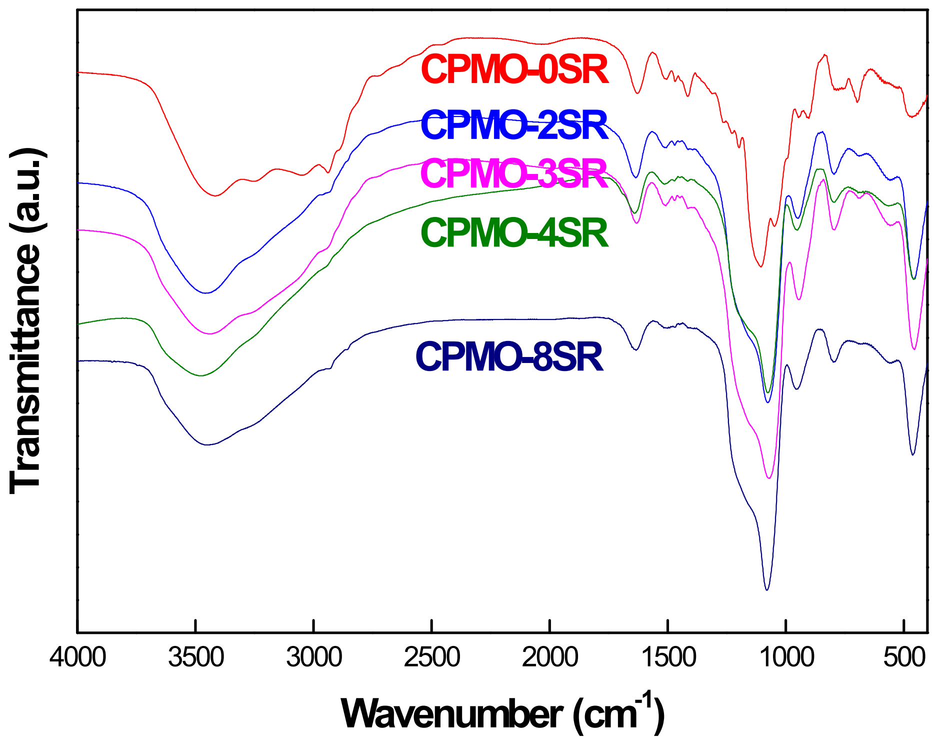

Figure S1. FT-IR of CPMOs

Table S1. Observed FT-IR band positions along with their assignments of CPMOs

Band assignments	Wavenumber (cm^{-1})
C-H stretching(APTES)	2929-2856
ν_{as} (P=N-P)	1406-1418
P=N	1196-1209
Si-O-Si and ν_{as} (P-NH-P)	1237-1050
ν_{as} (P-NH-P) and Si-OH	950
Si-O-Si	800
δ (P=N-P)	544-555

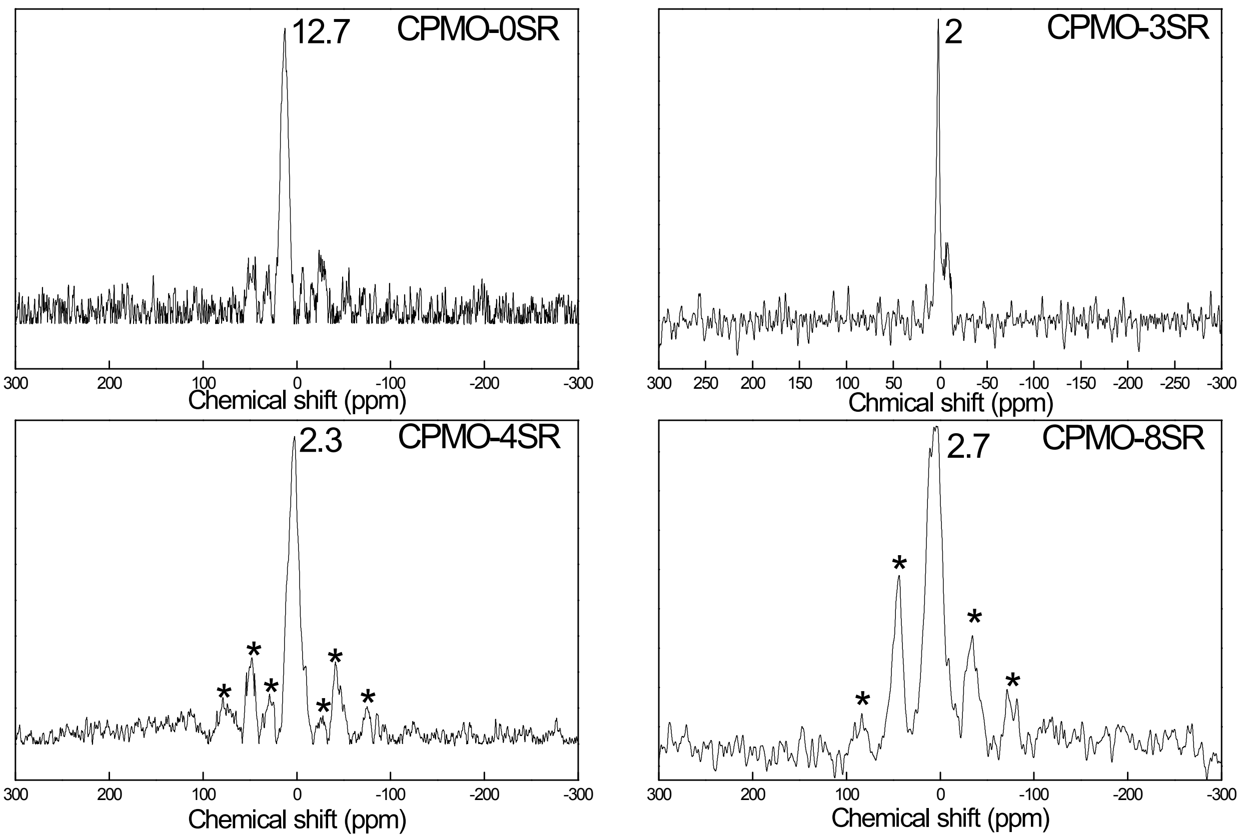

Figure S2. ^{31}P CPMAS NMR of CPMOs synthesized by sonication

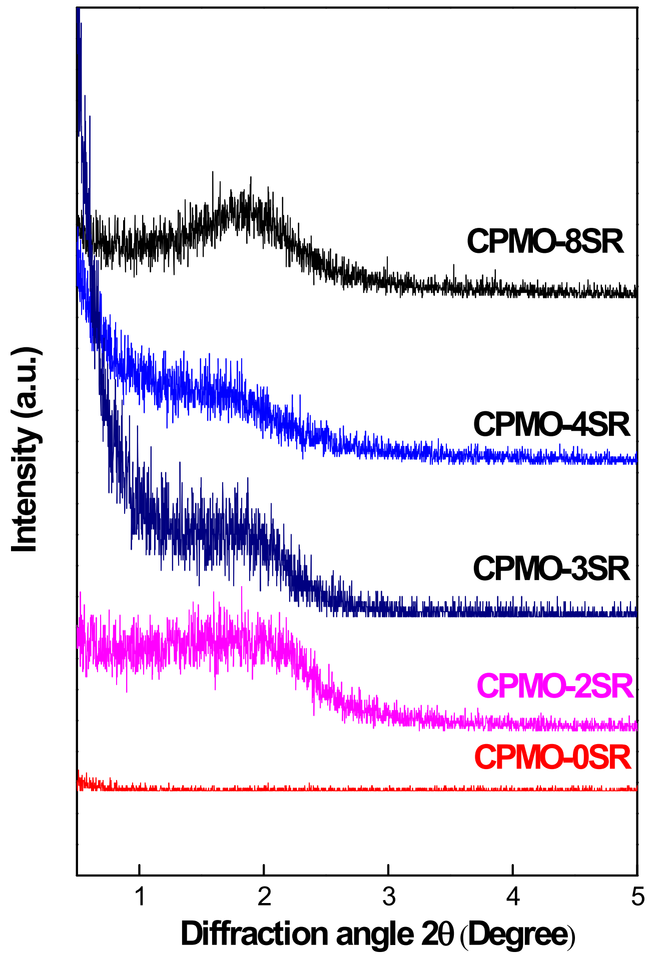

Figure S3. Small angle X-ray scattering pattern of CPMOs

Table S2. Position and % of the *T* and *Q* sites in different samples

Sample ID	Position of *T* sites		Position of *Q* sites		
	T^2 (ppm), (%)	T^3 (ppm), (%)	Q^2(ppm), (%)	Q^3 (ppm), (%)	Q^4 (ppm), (%)
CPMO-0SR	-58, (27.6)	-66, (72.4)	--	--	--
CPMO-4SR	-57, (20.1)	-66, (8.4)	-90, (8.1)	-100, (47.9)	-110, (15.5)

Table S3. C, H and N elemental analysis of CPMOs

Sample ID	N (wt%)	C (wt%)	H (wt%)	C/N ratio
CPMO-0SR	11.71	23.62	5.28	2.01
CPMO-2SR	6.19	11.85	3.17	1.91
CPMO-3SR	5.22	9.58	3.13	1.83
CPMO-4SR	5.14	8.93	2.85	1.73
CPMO-8SR	4.86	8.28	2.1	1.70

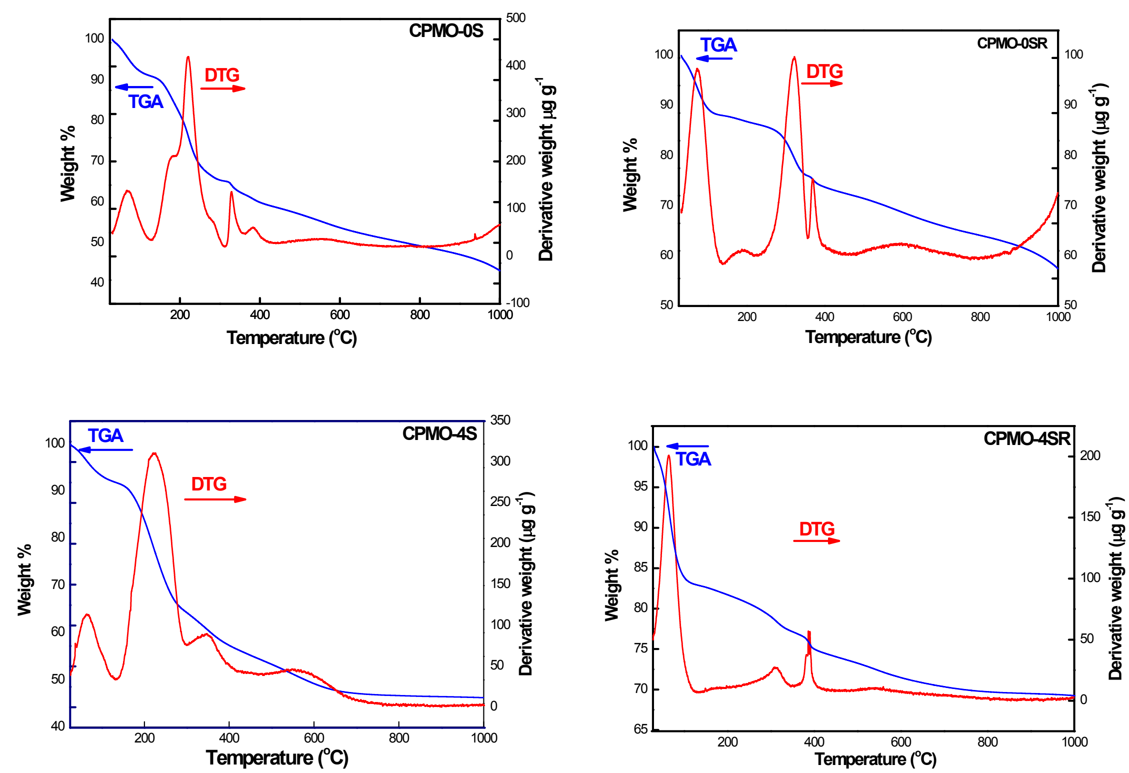

Figure S4. TGA and DTG thermograms of CPMOs measured in nitrogen atmosphere with a heating rate of 10 °C min^{-1}

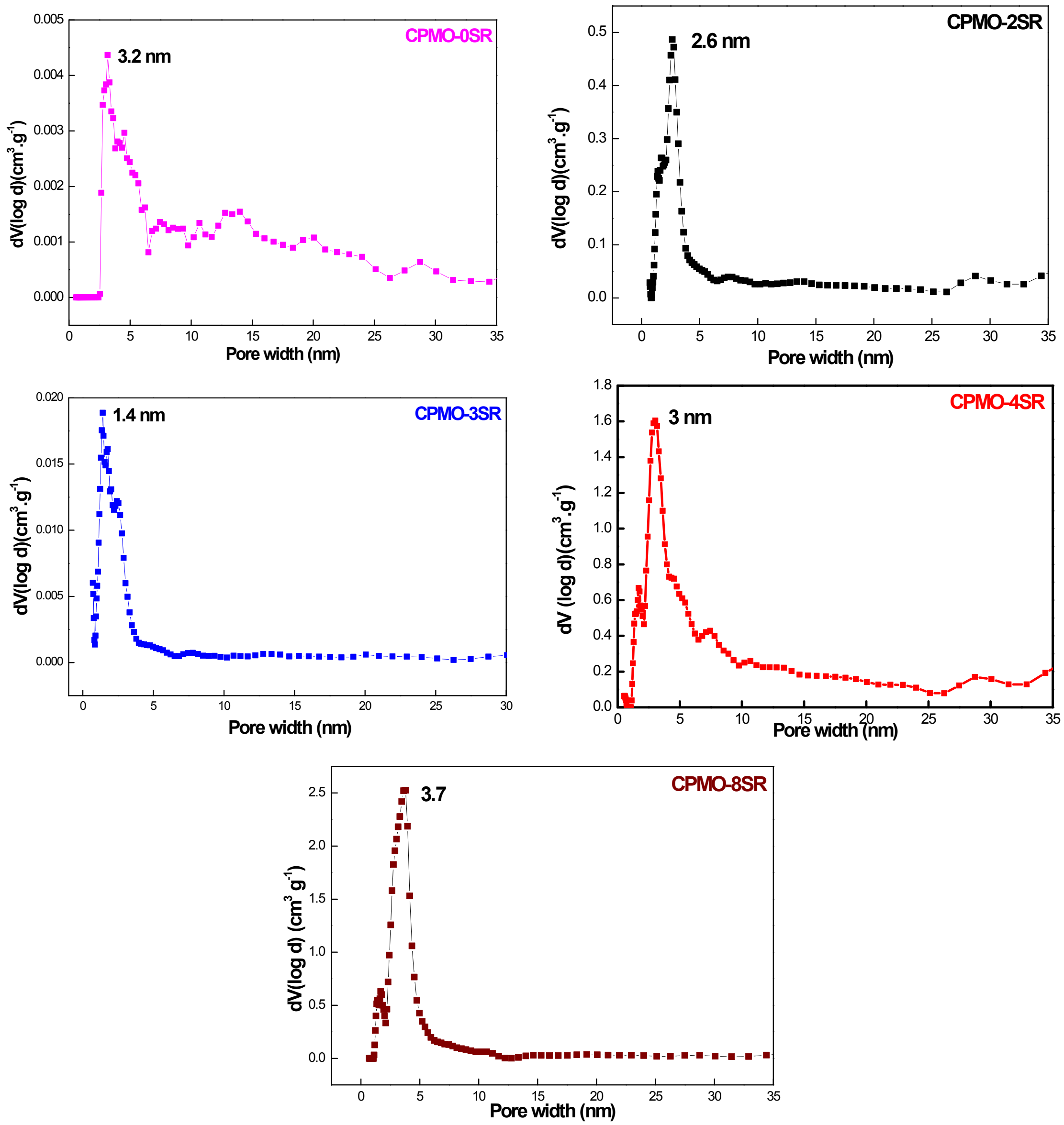

Figure S5. Pore size distribution of CPMOs

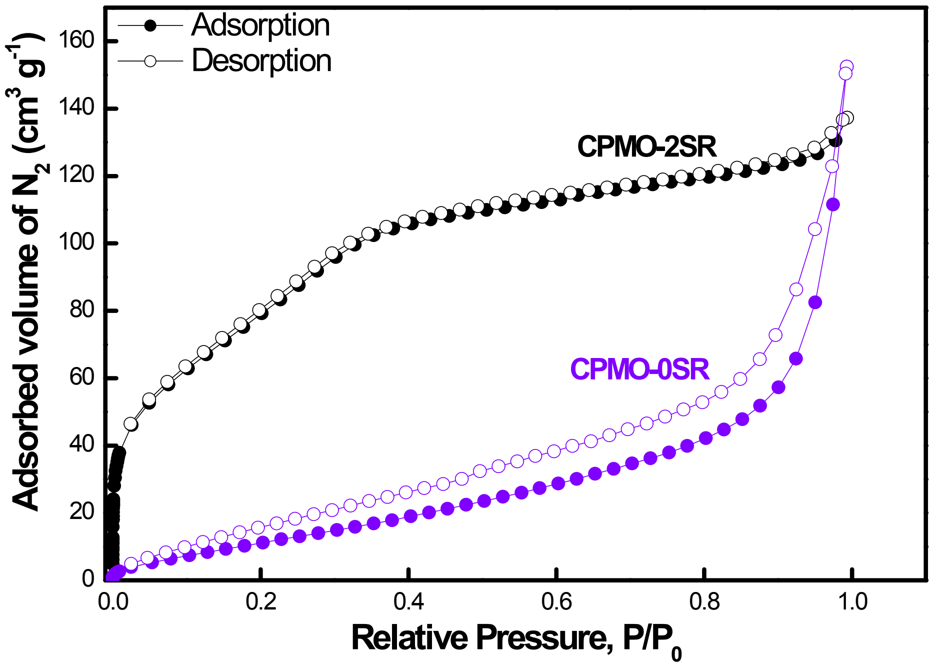

Figure S6. N_2 sorption isotherms of CPMO-0SR and CPMO-4SR measured at 77 K

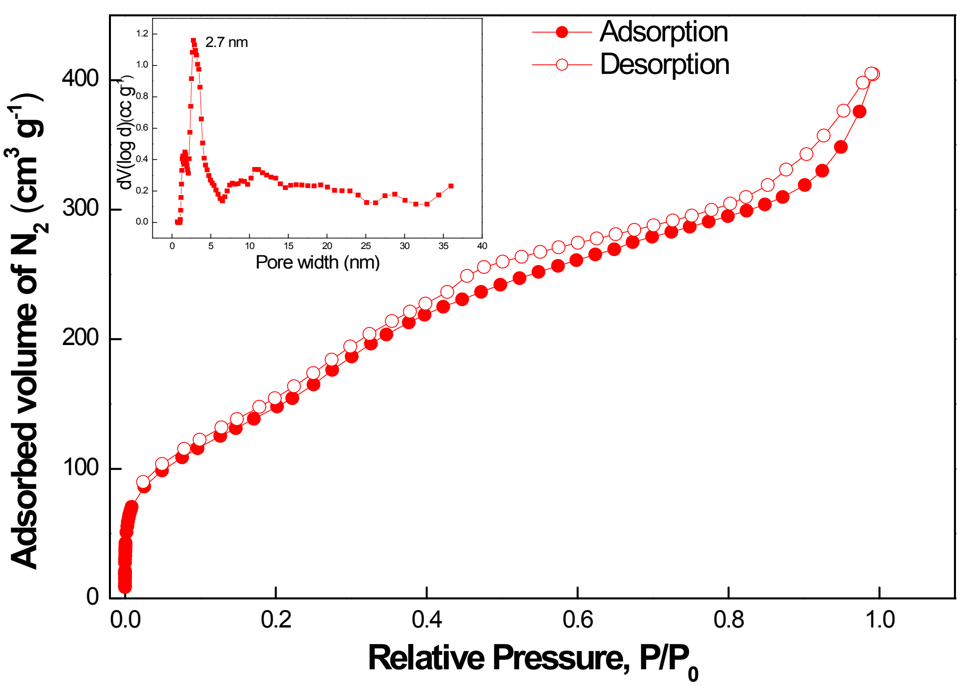

Figure S7. N_2 sorption isotherm of PMO-4S (without PNC) measured at 77 K

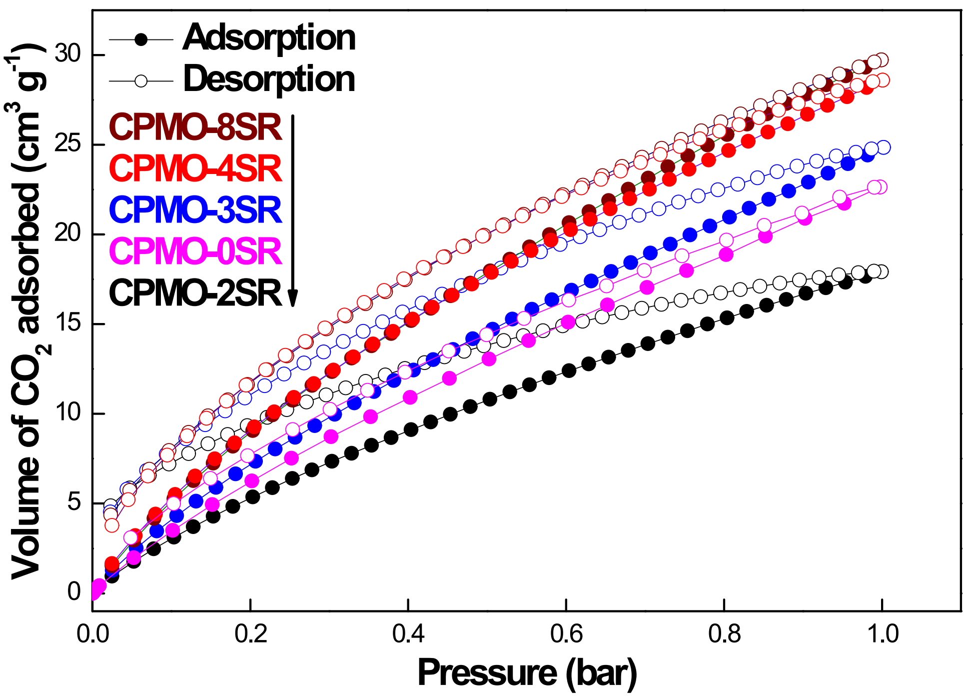

Figure S8. CO_2 sorption isotherms of CPMOs measured at 273K

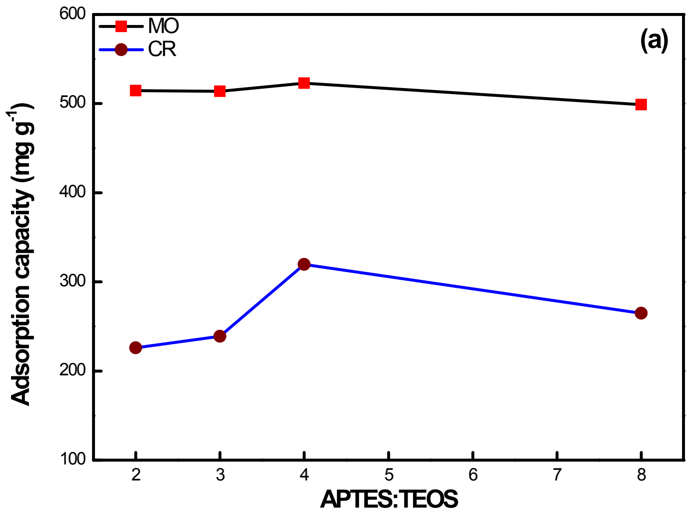

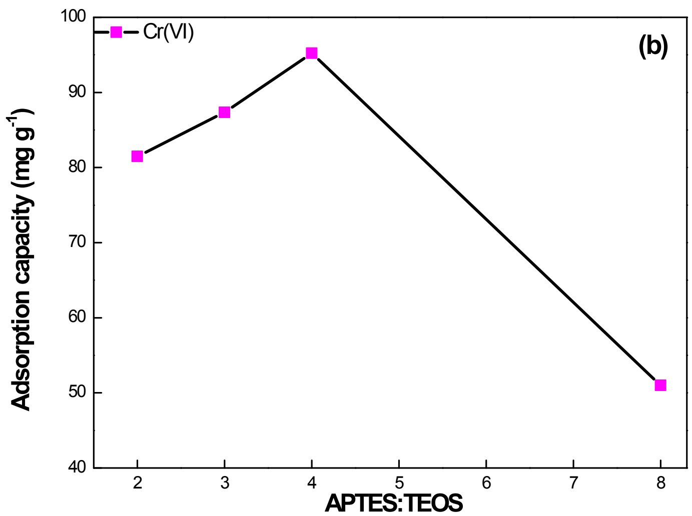

Figure S9. Comparison of adsorption capacity of CPMOs for (a) organic dyes and (b) Cr(VI) ions removal

Table S4. Comparison of adsorption capacities of CPMOs for (a) organic dyes and (b) Cr(VI) ions removal

Sample ID	MO (q_{max})(mg g^{-1})	CR (q_{max})(mg g^{-1})	Cr(VI)(q_{max})(mg g^{-1})
CPMO-2SR	514.515	226	81.469
CPMO-3SR	513.857	239	87.338
CPMO-4SR	523	319.46	95.206
CPMO-8SR	498.817	264.79	51
PMO-4S	474.307	281.32	73.3

Table S5: Adsorption capacities q_{max} for Cr (VI) removal of selected results from the literature

Silica type	q_{max} (mg g^{-1})	Ref.
3 Aminopropyl functionalized MCM-48	65	S1
6-amino-4-azahexyl functionalized MCM-48	119	S1
9-amino-4,7-diazanonyl functionalized MCM-48	160	S1
AP-TMS modified MCM-45	40	S2
Amine-Functionalized Mesoporous Silica	82	S3
Magnetic functionalized MCM-48 mesoporous silica with melamine	115.6	S4
CPMO-4SR	**101**	**Present work**

Table S6: Adsorption capacities q_{max} for methyl orange removal of selected results from the literature

Material type	q_{max} (mg g^{-1})	Ref.
Ammonium-functionalized silica nanoparticle	105.4	S5
Mesoporous carbon material	294.1	S6
Alkali-activated multiwalled carbon nanotubes	149	S7
Poly HEMA–chitosan-MWCNT nano-composite	306	S8
CPMO-4SR	**523**	**Present work**

Table S7: Adsorption capacities q_{max} for congo red removal of selected results from the literature

Silica type	q_{max} (mg g^{-1})	Ref.
Modified xanthan gum/silica hybrid nanocomposite	209.21	S9
Graphene oxide/chitosan fibers	294.12	S10
Maghemite nanoparticles	208.33	S11
Cu-BTC	959.9	S12
Ni50/Cu-BTC	1078	S12
CPMO-4 SR	**320**	**Present work**

Table S8. Thermodynamic parameters for the adsorption of organic dyes and Cr(VI) ions by CPMO-4SR

MO		CR	Cr(VI) ion
T (K)	ΔG (kJ mol^{-1})	ΔG (kJ mol^{-1})	
283	--	-0.292	--
293	-8.095	-0.312	--
298	-8.254	-0.324	-7.4
303	-8.384	-0.321	--
313	-8.635	-0.326	-5.089
323	-8.80	-0.304	--
333	-9.04	-0.301	-1.58
343	--	-0.289	--
353	--	-0.256	--

Table S9. Thermodynamic parameters for the adsorption of organic dyes and Cr(VI) ions by CPMO-4SR

Adsorbate	Thermodynamic parameters	
	Δ H(kJ mol^{-1})	ΔS [J (mol K)$^{-1}$)]
MO	-1.377	23
CR	-0.461	-0.498
Cr(VI) ion	-7.096	-172

References

S1. T. Yokoi, Y. Kubota and T. Tatsumi, *Appl. Catal. A*, 2012, **421– 422**, 14-37.

S2. S. A. Idris, K. M. Alotaibi, T. A. Peshkur, P. Anderson and M. Morris, *Microporous Mesoporous Mater.*, 2013, **165,** 99-105.

S3. X. Li, C. Han, W. Zhu, W. Ma, Y. Luo, Y. Zhou, J. Yu and K. Wei, *J. Chem.*, 2014, **2014,** 1-10.

S4. M. Anbia, K. Kargosha and S. Khoshbooei, *Chem. Eng. Res. Des.*, 2015, **93**, 779-788.

S5. J. Liu, S. Ma and L. Zang, *Appl. Surf. Sci.*, 2013**, 265**, 393– 398.

S6. N. Mohammadi, H. Khani, V. K. Gupta, E. Amereh and S. Agarwal, *J. Colloid Interface Sci.*, 2011, **362**, 457–462.

S7. J. Ma, F. Yu, L. Zhou, L. Jin, M. Yang, J. Luan, Y. Tang, H. Fan, Z. Yuan and J. Chen, *ACS Appl. Mater. Interfaces*, 2012, **4**, 5749−5760.

S8. H. Mahmoodian, O. Moradi, B. Shariatzadeha, T. A. Salehf, I. Tyagi, A. Maity, M. Asif, and V. K. Gupta, *J. Mol. Liq.*, 2015, **202**, 189–198.

S9. S. Ghorai, A. K. Sarkar, A. B. Panda and S. Pal, *Bioresour. Technol.*, 2013, **144,** 485–491.

S10. Q. Du, J. Sun, Y. Li, X. Yang, X. Wang, Z. Wang and L. Xia, *Chem. Eng. J.,* 2014, **245**, 99–106.

S11. A. Afkhami and R. Moosavi, *J. Hazard. Mater.,* 2010, **174**, 398–403.

S12. J. Hu, H. Yu, W. Dai, X. Yan, X. Hu and H. Huang, *RSC Adv.,* 2014, **4**, 35124–35130.